Strauss, E., Zhai, H., Brand, L.A., McLafferty, F.W. & Begley, T.P. Mechanistic studies on phosphopantothenoylcysteine decarboxylase: trapping of an enethiolate intermediate with a...

ARTICLE *in* BIOCHEMISTRY · JANUARY 2005

Impact Factor: 3.02 · DOI: 10.1021/bi048340a · Source: PubMed

5 AUTHORS, INCLUDING:

Erick Strauss
Stellenbosch University
38 PUBLICATIONS **867** CITATIONS

Mechanistic Studies on Phosphopantothenoylcysteine Decarboxylase: Trapping of an Enethiolate Intermediate with a Mechanism-Based Inactivating Agent†

Erick Strauss,*,§ Huili Zhai,‡ Leisl A. Brand,§ Fred W. McLafferty,‡ and Tadhg P. Begley*,‡

Department of Chemistry and Chemical Biology, Baker Laboratory, Cornell University, Ithaca, New York 14853, and Department of Chemistry, University of Stellenbosch, Private Bag X1, Matieland 7602, South Africa

Received August 3, 2004; Revised Manuscript Received September 26, 2004

ABSTRACT: Phosphopantothenoylcysteine decarboxylase (*P*PC-DC) catalyzes the decarboxylation of the cysteine moiety of 4′-phosphopantothenoylcysteine (*P*PC) to form 4′-phosphopantetheine (*P*PantSH); this reaction forms part of the biosynthesis of coenzyme A. The enzyme is a member of the larger family of cysteine decarboxylases including the lantibiotic-biosynthesizing enzymes EpiD and MrsD, all of which use a tightly bound flavin cofactor to oxidize the thiol moiety of the substrate to a thioaldehyde. The thioaldehyde serves to delocalize the charge that develops in the subsequent decarboxylation reaction. In the case of *P*PC-DC enzymes the resulting enethiol is reduced to a thiol giving net decarboxylation of cysteine, while in EpiD and MrsD it is released as the final product of the reaction. In this paper, we describe the characterization of the novel cyclopropyl-substituted product analogue 4′-phospho-*N*-(1-mercaptomethyl-cyclopropyl)-pantothenamide (*P*PanΔSH) as a mechanism-based inhibitor of the human *P*PC-DC enzyme. This inhibitor alkylates the enzyme on Cys^{173}, resulting in the trapping of a covalently bound enethiolate intermediate. When Cys^{173} is exchanged for the weaker acid serine by site-directed mutagenesis the enethiolate reaction intermediate also accumulates. This suggests that Cys^{173} serves as an active site acid in the protonation of the enethiolate intermediate in *P*PC-DC enzymes. We propose that this protonation step is the key mechanistic difference between the oxidative decarboxylases EpiD and MrsD (which have either serine or threonine at the corresponding position in their active sites) and *P*PC-DC enzymes, which also reduce the intermediate in an overall simple decarboxylation reaction.

Phosphopantothenoylcysteine decarboxylase (*P*PC-DC)[1] catalyzes the decarboxylation of the cysteine moiety of 4′-phosphopantothenoylcysteine (**1**, *P*PC) to form 4′-phosphopantetheine (**2**, *P*PantSH) (Scheme 1) (*1*). In *Escherichia coli* and most other prokaryotes (with the exception of the Enterococci and Streptococci), this activity is fused with another enzyme bearing phosphopantothenoylcysteine synthetase (*P*PC-S) activity to form a bifunctional enzyme (CoaBC). In contrast, *P*PC-DC enzymes in eukaryotic systems, including *Arabidopsis thaliana* (*2*) and the recently identified human enzyme (*3*), are monofunctional. Both of these activities form part of the biosynthetic machinery that converts pantothenate (vitamin B_5) into coenzyme A (CoA), an essential cofactor in all living systems.

Scheme 1

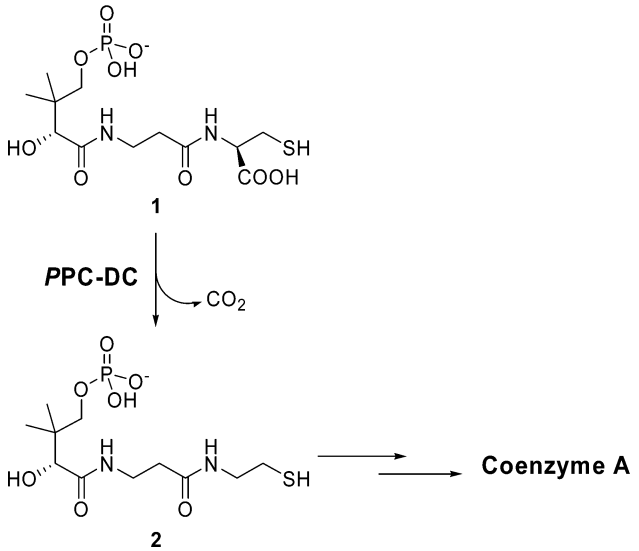

*P*PC-DC utilizes a flavin cofactor (FMN) for catalysis (*4*, *5*). This suggests a mechanism for the decarboxylation in

† This research was supported by a grant from the Petroleum Research Fund of the ACS, a gift from GlaxoSmithKline to T.P.B. and by a grant from Stellenbosch University to E.S.

* To whom correspondence should be addressed. For E.S.: tel +27-21-808-3355; fax +27-21-808-3360; e-mail estrauss@sun.ac.za. For T.P.B.: tel 607-255-7133; fax 607-255-4137; e-mail tpb2@cornell.edu.

§ University of Stellenbosch.

‡ Cornell University.

[1] Abbreviations: *P*PC-DC, 4′-phosphopantothenoylcysteine decarboxylase; *P*PC, 4′-phosphopantothenoylcysteine; *P*PantSH, 4′-phosphopantetheine; *P*PC-S, 4′-phosphopantothenoylcysteine synthetase; CoA, coenzyme A; FMN, flavin mononucleotide (oxidized); $FMNH^-$, flavin mononucleotide (reduced); AtHAL3a, *P*PC-DC from *Arabidopsis thaliana*; *P*PanΔSH, 4′-phospho-*N*-(1-mercaptomethyl-cyclopropyl)-pantothenamide; ACC, 1-amino-1-cyclopropanecarboxylic acid; FTMS, Fourier transform mass spectroscopy; HsCoaC, *P*PC-DC from *Homo sapiens*; Lys-C, Lys-C endoproteinase; Glu-C, Glu-C endoproteinase; NADH, nicotinamide dinucleotide (reduced); NMR, nuclear magnetic resonance; ESI-MS, electrospray ionization mass spectroscopy; THF, tetrahydrofuran; LB, Luria-Bertani broth; OD_{600}, optical density at 600 nm; IPTG, isopropyl-β-D-thiogalactopyranoside; DTT, dithiothreitol; Tris-HCl, tris(hydroxymethyl)aminomethane hydrochloride; rTEV, recombinant tobacco etch virus; PCR, polymerase chain reaction; *P*PAT, 4′-phosphopantetheine adenylyltransferase; MeOH, methanol; AcOH, acetic acid; DIPEA, *N*,*N*-diisopropylethylamine.

10.1021/bi048340a CCC: $27.50
Published on Web 11/12/2004

Scheme 2 [a]

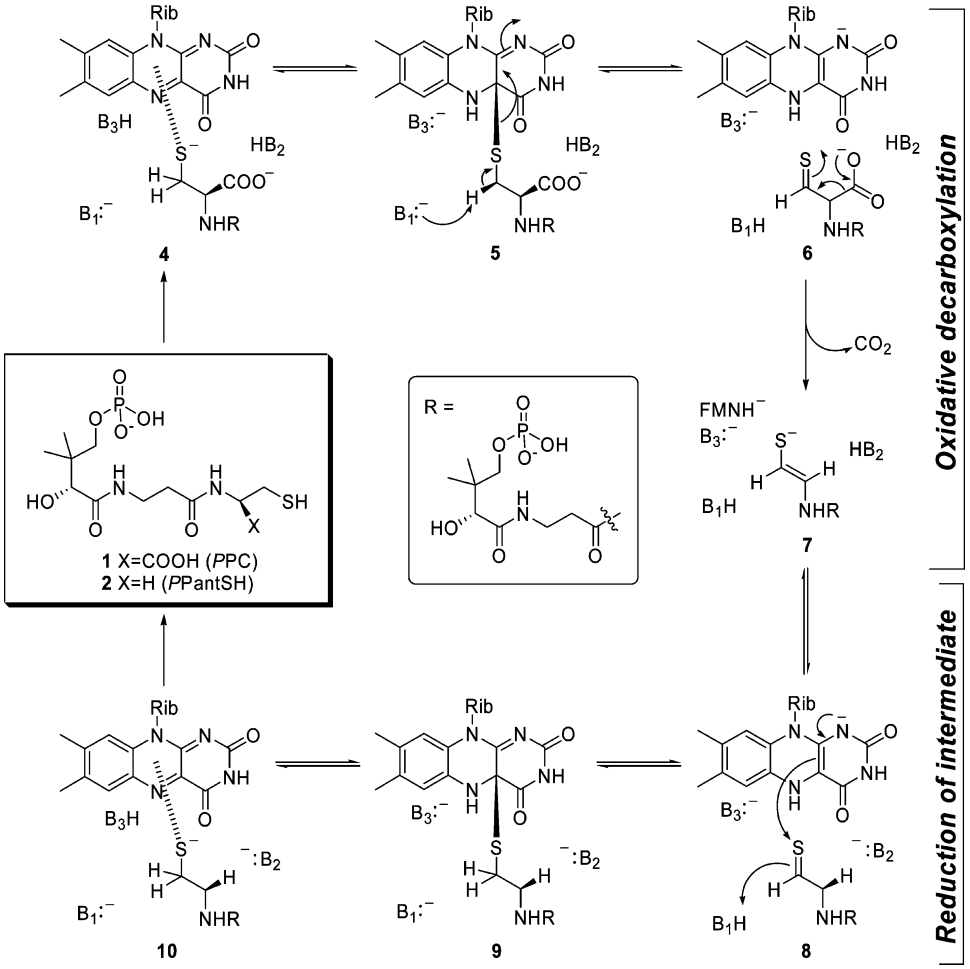

[a] R = 4′-Phosphopantothenoyl (shown in center box) throughout the paper.

which flavin oxidizes the thiol of **1** to a thioaldehyde intermediate (**6**); this thioaldehyde allows the delocalization of the charge that develops during the decarboxylation reaction (Scheme 2). Reduction of the resulting enethiolate **7** by the reduced flavin cofactor completes the reaction. This mechanism is consistent with our previous observations that the decarboxylation proceeds with retention of stereochemistry and that the pro-*R* proton at C_β of the cysteine moiety is reversibly removed during the reaction while the proton at C_α is not involved (*4*, *6*). Furthermore, the observation of both substrate- and product-induced thiolate−flavin charge-transfer complexes supports the formation of intermediates **4** and **10** (*4*). Such charge-transfer complexes have been observed as long-wavelength absorptions in the flavin spectra of several enzymes involved in thiol redox chemistry, such as mercuric ion reductase and lipoamide dehydrogenase (*7*−*9*). In each of these enzymes, the thiolate−flavin charge-transfer complex is in equilibrium with a flavin C(4a)−thiol adduct.

In combination, these results argue against a mechanism involving direct hydride transfer from the substrate to the flavin during oxidation, while supporting the formation of the flavin C(4a)−thiol adducts **5** and **9** as intermediates in both the oxidation and reduction steps.

EpiD (*10*, *11*) and MrsD (*12*) are flavin-dependent lantibiotic-biosynthesizing enzymes that catalyze the oxidative decarboxylation of peptidyl-cysteine residues (**11**) to

Scheme 3

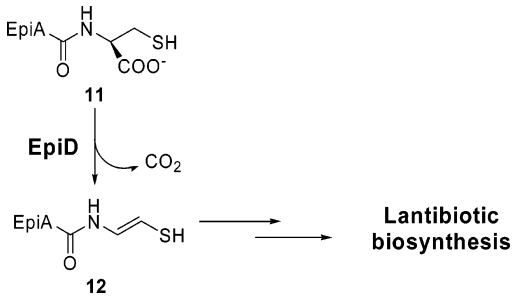

form peptidyl-aminoethenethiol products (**12**) (Scheme 3). In contrast to *P*PC-DC these enethiol products are not reduced but released to serve as substrates in subsequent reactions in lantibiotic biosynthesis (*13*). A mechanistic explanation for the different activities of these related enzymes is currently lacking.

The structures of EpiD and *A. thaliana P*PC-DC (AtHAL3a) have been determined, and the active sites of both enzymes have been extensively mapped by mutagenesis (*5*, *14*−*17*). The AtHAL3a C175S mutant was particularly interesting because it gave the enethiol as the exclusive reaction product (*14*). Subsequently the structure of this mutant enzyme with bound dephospho-**7** was solved and showed that Cys^{175} forms part of a binding clamp, which is in close contact with the substrate (*18*). The location of this residue at the active site as well as the truncated activity of the C175S mutant

Scheme 4

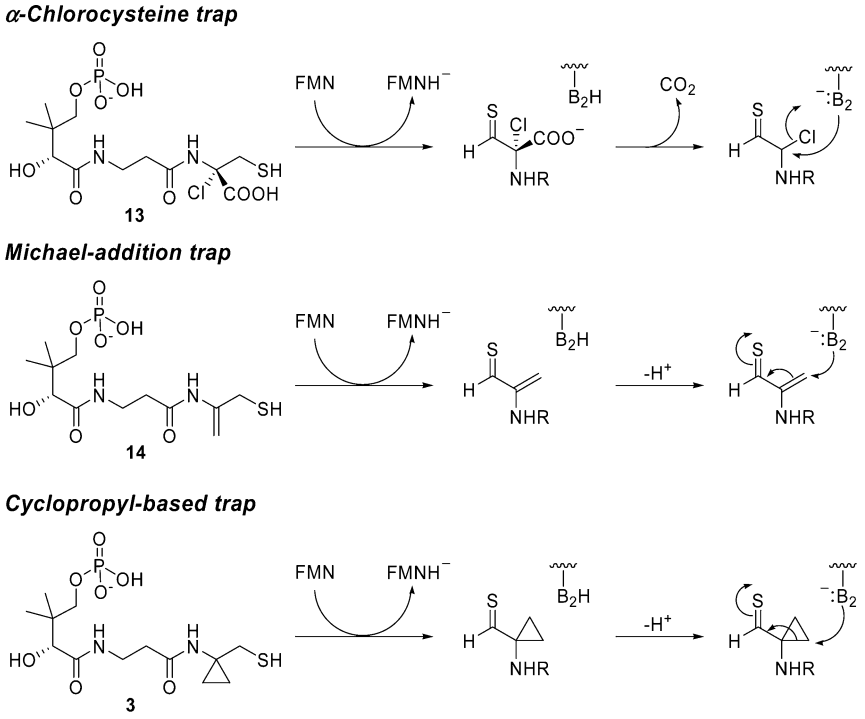

suggested that Cys[175] plays an important role in the catalysis of the reduction of the enethiolate **7**. The mechanistic proposal outlined in Scheme 2 requires that **7** must be protonated to give **8** before reduction can take place. The mutagenesis and structure both point to Cys[175] as the proton donor (B_2H in Scheme 2) for this reaction. This analysis is also supported by the observation that the active site cysteine residue of *P*PC-DC is replaced with the less acidic serine and threonine residues in the enethiol-forming enzymes EpiD and MrsD (*17*).

To further probe the role of this active site cysteine, we designed a substrate analogue to alkylate any nucleophile positioned close to C_α of the enethiolate **7** (such as the deprotonated B_2H shown in Scheme 2). We considered the three alkylation strategies shown in Scheme 4. We rejected the first strategy because it is likely that α-chloro-substituted substrates (**13**) would be unstable and could alkylate the enzyme prior to thiol oxidation. We rejected the second strategy, which is based on the use of masked Michael acceptors such as **14**, since *N*-vinyl amides are difficult to prepare and are also prone to polymerization. We decided to implement the third strategy in our study and use the cyclopropyl-containing product analogue 4′-phospho-*N*-(1-mercaptomethyl-cyclopropyl)-pantothenamide (*P*PanΔSH (**3**)). This compound is likely to be active site selective because it requires oxidation to the corresponding thioaldehyde before nucleophilic attack can occur. In addition, *P*PanΔSH (**3**) should be stable in an aqueous environment and can be prepared by a relatively uncomplicated synthetic route.

Analogous nucleophilic ring-opening reactions of activated cyclopropyl groups are encountered in various organic syntheses and also in the study of enzyme mechanisms. For example, the nucleophilic ring opening of the cyclopropyl group of 1-amino-1-cyclopropanecarboxylic acid (ACC) occurs when the substrate is activated by imine formation with a pyridoxal cofactor in a reaction catalyzed by ACC deaminase (*19*−*22*). Activated cyclopropyl-containing substrate analogues are also used as electrophilic traps in a wide variety of enzyme-catalyzed reactions (*23*−*32*), while nucleophilic ring opening of cyclopropanes substituted with two ester groups has been extensively used in organic synthesis (*33*). In all these cases, the ring-opening reaction is driven by the strain in the cyclopropyl ring and by the stabilization of the resulting carbanion by electron-withdrawing substituents (such as esters or aldehydes) on the ring. The observation that a thioaldehyde group is more effective at stabilizing an adjacent carbanion than two esters (the estimated pK_a of enethiolate **7** is 6.0 (*34*) compared to the pK_a of diethyl malonate at ∼13) suggested that the cyclopropyl-containing **3** would be an efficient trap of active site nucleophiles in *P*PC-DC.

In this paper, we describe the synthesis of *P*PanΔSH (**3**) and its characterization as a mechanism-based inhibitor of human *P*PC-DC and combine it with an analysis of the reactivity of the *P*PC-DC C173S mutant to further elucidate the catalytic role of the active site cysteine.

EXPERIMENTAL PROCEDURES

Materials and Methods. All chemicals were from Aldrich, Sigma, or Acros Organics and were of the highest purity available. Endoproteinase Lys-C and endoproteinase Glu-C were from Sigma and were used without further purification. 4′-Phosphopantetheine (**2**, *P*PantSH) was synthesized as previously described (*35*), while 4′-phosphopantothenoylcysteine (**1**, *P*PC) was prepared from *S*-ethyl thiopantothenate 4′-*O*,*O*-dibenzyl phosphate (**18**) using a previously published synthesis (*36*). A molar extinction coefficient of 6220 $M^{-1}\cdot cm^{-1}$ was used for NADH in all kinetic analyses. A Hitachi U-2010 spectrophotometer was used for all kinetic experiments, while absorption spectra were recorded on a ThermoSpectronic Helios Alpha instrument. A Varian INOVA 400 MHz instrument was used for ^1H NMR spectros-

copy. ESI-MS analyses were performed either at the Cornell Biotechnology Resource Center on a Bruker Esquire-LC ESI-ion trap mass spectrometer by direct infusion of the analyte mixture into the instrument at a rate of 1 μL/min or at the Central Analytical Facility at Stellenbosch University on a Waters Micromass Q-TOF Ultima API mass spectrometer. DNA sequencing was performed at Inqaba Biotec (Pretoria, South Africa). For ease of comparison between *P*PC-DC enzymes from other sources, the numbering of the amino acid residues of the human CoaC protein was done according to the sequence of the native enzyme, as shown in Figure 5.

*N-(1-Hydroxymethyl-cyclopropyl)-thioacetamide (**16**).* A suspension of ACC (**15**) (242 mg, 2.47 mmol) in 2 mL of dry THF was stirred under argon at room temperature, followed by slow addition of 10 mL of a 1.0 M solution of BH_3 in THF (10 mmol). The mixture was subsequently refluxed overnight. After the solution was cooled to 0 °C in an ice bath, methanol (1.22 mL, 30 mmol) was carefully added. The solution was stirred for 30 min before 1.0 M HCl (2.47 mL, 2.47 mmol) was added, causing a precipitate to form. The solvent was removed, and the precipitate was dried by rotoevaporation. The resulting residue was dissolved in 3.5 mL of methanol, and DIPEA (627 μL, 3.60 mmol) and ethyldithioacetate (413 μL, 3.60 mmol) were added. The solution was then refluxed for 4 h. The solvent was removed by rotoevaporation, and the residue was purified by flash column chromatography (silica gel; MeOH/CH_2Cl_2, 2:98 to 4:96) to give **16** as a clear oil (241 mg, 67%). ^{1}H NMR (400 MHz, $CDCl_3$): δ 1.02 (s, 4H), 2.51 (s, 3H), 3.81 (s, 2H), 7.78 (b, 1H).

*5-Methyl-6-thia-4-aza-spiro[2.4]hept-4-ene (**17**).* A solution of **16** (236 mg, 1.63 mmol) in 25 mL of dry CH_2Cl_2 was cooled to −20 °C (dry ice/acetonitrile), and [bis(2-methoxyethyl)amino]sulfur trifluoride (Deoxo-Fluor) (357 μL, 1.95 mmol) was added in six portions over 20 min, maintaining the temperature at −20 °C. The mixture was stirred for a further 40 min at −20 °C, after which 10 mL of saturated $NaHCO_3$ was added to quench the reaction. The reaction mixture was allowed to warm to room temperature and then extracted with CH_2Cl_2 (2 × 25 mL). The organic extracts were combined and dried over $MgSO_4$, and the solvent was removed by rotoevaporation. The residue was purified by flash column chromatography (silica gel; ethyl acetate/hexane, 1:3) to give **17** as a clear oil (77 mg, 37%). ^{1}H NMR (400 MHz, $CDCl_3$): δ 0.83 (s, 2H), 1.31 (s, 2H), 2.24 (s, 3H), 3.38 (s, 2H).

*S-Ethyl Thiopantothenate 4′-O,O-Dibenzyl Phosphate (**18**).* Dibenzylchlorophosphate was prepared in situ by reacting dibenzyl phosphite (tech., 85%; 1.97 g, 6.0 mmol) and *N*-chlorosuccinimide (0.80 g, 6.0 mmol) in dry benzene (8 mL) for 2 h at room temperature. The reaction mixture was filtered to remove the succinimide, and the filtrate was added dropwise to a solution of *S*-ethyl thiopantothenate (527 mg, 2.0 mmol) (*6*) in dry pyridine (9 mL) at −40 °C (dry ice/acetonitrile). After stirring at −40 °C for 2 h, the mixture was placed in a −20 °C freezer overnight. The reaction was then allowed to warm to room temperature and was quenched with water (3 mL). The solvent was removed by rotoevaporation, and ethyl acetate (50 mL) was added. The resulting suspension was washed with 1 M H_2SO_4 (2 × 10 mL), 1 M $NaHCO_3$ (2 × 10 mL), and saturated Na_2SO_4 (1 × 10 mL). The organic layer was dried over Na_2SO_4, and the solvent was removed. The product was purified by flash column chromatography (silica gel; ethyl acetate/hexane, 3:1) to give **18** as a colorless oil (769 mg, 73% yield). ^{1}H NMR (400 MHz, $CDCl_3$): δ 0.75 (s, 3H), 1.05 (s, 3H), 1.22 (t, 3H), 2.86 (t, 2H), 2.78 (q, 2H), 3.45−3.56 (m, 3H), 3.88 (s, 1H), 4.03 (t, 1H), 4.96−5.05 (m, 4H), 7.29−7.36 (arom, 10H).

*N-(1-Mercaptomethyl-cyclopropyl)-pantothenamide 4′-O,O-Dibenzyl Phosphate (**19**).* A solution of **17** (76 mg, 597 μmol) in 5 mL of 2.5 M HCl was heated to 100 °C overnight. After the mixture cooled to room temperature, the solvent was evaporated; the residue was dissolved in H_2O and then lyophilized. The resulting residue was suspended in 1.5 mL of methanol, and DIPEA (123 μL, 705 μmol) was added. A solution of **18** (369 mg, 705 μmol) in 2.0 mL of methanol was subsequently added to the mixture, and the resulting solution was refluxed for 3 h. The solvent was removed by rotoevaporation, and the residue was resuspended in 25 mL of ethyl acetate. The solution was sequentially washed with 1 M H_2SO_4 (2 × 5 mL), 1 M $NaHCO_3$ (2 × 5 mL), and saturated NaCl (1 × 5 mL). The organic layer was dried over Na_2SO_4, and the solvent was removed. The residue was purified by flash column chromatography (silica gel; MeOH/CH_2Cl_2, 2:98 to 5:95) to give **19** as a clear oil (121 mg, 37%). ^{1}H NMR (400 MHz, $CDCl_3$): δ 0.76 (s, 2H), 0.78 (s, 3H), 0.84 (s, 2H), 1.04 (s, 3H), 2.32−2.45 (m, 2H), 2.74 (dq, 2H), 3.52 (t, 2H), 3.88 (s, 1H), 3.89 (dd, 2H), 4.98−5.06 (m, 4H), 6.54 (b, 1H), 7.26 (b, 1H), 7.31−7.35 (arom, 10H).

*4′-Phospho-N-(1-mercaptomethyl-cyclopropyl)-pantothenamide (**3**).* A solution of **19** (114 mg, 202 μmol) in ∼5 mL of liquid NH_3 was treated with sodium pieces until the blue color persisted. Methanol (2 drops) was then added, and the ammonia was allowed to evaporate. Ice water (1 mL) was added, followed by a sufficient amount of Dowex 50WX8-100 resin suspended in deionized water to adjust the pH of the solution to below 3.5. The suspension was loaded on a Dowex 50WX8-100 column (500 μL) prepared in a plastic pipet and equilibrated with deionized water. The product was eluted with 2 mL of water and recovered by lyophilization of the eluate to give **3** as a clear glass (78 mg, quantitative). The final product was dissolved in H_2O, titrated to pH ∼6.5 with 1 M NaOH, and stored as frozen aliquots of a stock solution (100 mM) at −20 °C. ^{1}H NMR (400 MHz, D_2O): δ 0.62−0.66 (m, 4H), 0.69 (s, 3H), 0.77 (s, 3H), 2.25 (t, 2H), 2.51 (s, 1H), 2.81 (s, 1H), 3.29 (t, 2H), 3.42 (dd, 1H), 3.62 (dd, 1H), 3.82 (d, 1H). ESI-MS: $[M + H]^+$ calcd for $C_{13}H_{26}N_2O_7PS$ *m*/*z* 385.12, found 385.15.

*4′-Phosphopantothenate (**30**).* Benzyl pantothenate 4′-*O*,*O*-dibenzyl phosphate (*36*) (419 mg, 736 mmol) was dissolved in 4.4% formic acid in methanol (21 mL), and palladium black (210 mg) was added. The mixture was stirred at room temperature for 30 min. The catalyst was removed by filtration, washing the residue with 10 mL methanol and 10 mL water. [CAUTION: Catalyst allowed to dry on filter paper will ignite in air.] The solvent was removed from the combined filtrates in vacuo. The residue was subsequently dissolved in water and lyophilized to give **30** as a clear glass (251 mg, >100%). The product was dissolved in H_2O, titrated to pH ∼6.5 with 1 M NaOH, and stored as frozen aliquots of a stock solution (50 mM) at −20 °C. ^{1}H NMR (400 MHz, D_2O): δ 0.70 (s, 3H), 0.77 (s, 3H), 2.43 (t, 2H),

3.31 (t, 2H), 3.43−3.45 (m, 1H), 3.64 (d of d, 1H), 3.82 (s, 1H).

Enzyme Purification and Handling. Human *P*PC-DC (HsCoaC) has previously been cloned and overexpressed in *E. coli* BL21 as an N-terminal hexahistidine fusion protein (6×His-HsCoaC) (*3*). To obtain pure protein, *E. coli* BL21 cells containing the plasmid pPROEX-HTa-HscoaC were grown at 37 °C in 500 mL of LB supplemented with 200 μg/mL ampicillin to $OD_{600} \approx 0.6$ and induced with 0.8 mM IPTG. After growing overnight at 37 °C, the cells were harvested, suspended in sonication buffer (5 mM imidazole, 500 mM NaCl, and 20 mM Tris-HCl, pH 7.9, 10 mL/g cell paste), and disrupted by sonication. The cell-free extract was clarified by centrifugation (35 000 × *g* for 30 min) before application to a 2.5 mL His-Bind column (Novagen). Weakly bound proteins were removed by washing with sonication buffer, followed by sonication buffer containing 100 mM imidazole. HsCoaC was obtained by eluting with sonication buffer containing 500 mM imidazole. The protein was exchanged to Tris buffer (25 mM Tris-HCl, 5 mM $MgCl_2$, 5% glycerol, pH 8.0) using PD-10 gel filtration columns (Amersham Biosciences) and stored as aliquots at −80 °C.

For FTMS analysis, the N-terminal hexahistidine fusion was removed by treatment of a 220 μL solution of 6×His-HsCoaC (720 μg) in 50 mM Tris-HCl, 10 mM $MgCl_2$, and 1.0 mM DTT at pH 8.0 with rTEV protease (180 units, Invitrogen) for 3 h at 30 °C. The cleaved 6×His-tag was removed by adding 10 μL of a solution containing 7.0 M NaCl and 230 mM imidazole to the protease-treated mixture and loading it onto a 1.5 mL Ni-NTA column (Qiagen) equilibrated with Ni-NTA buffer (10 mM imidazole, 300 mM NaCl, and 50 mM Tris-HCl, pH 8.0). The protein was obtained by elution with Ni-NTA buffer.

HsCoaC C173S Mutant. To obtain the C173S mutant of the human *P*PC-DC enzyme, the plasmid pPROEX-HTa-HscoaC was used as a template (25 ng in 50 μL PCR reaction mixture) for site-directed mutagenesis using the QuickChange site-directed mutagenesis kit (Stratagene). Mutagenesis was affected by changing the codon ^{173}GCG to CCG, using the following primers (the introduced mutation is underlined): 5′-CCAAGAAGCTGGTGTCCGGAGATGAAGGTC-3′ (forward) and 5′-GACCTTCATCTCCGGACACCAGCTTCT-TGG-3′ (reverse). Antibiotic selection on LB-agar plates containing 200 μg/mL ampicillin resulted in the growth of a small number of colonies. The mutant plasmid (named pPROEX-HTa-HscoaC C173S) was purified from one such colony using the Wizard Plus SV miniprep DNA purification kit (Promega). The presence of the mutation was confirmed by DNA sequencing.

The mutant protein (6×His-HsCoaC C173S) was expressed and purified using the same procedure as described above. Upon purification, and even after buffer exchange by gel filtration, solutions of 6×His-HsCoaC C173S remained green.

*PPC-DC Assays. P*PC-DC activity was assayed by coupling to phosphopantetheine adenylyltransferase (*P*PAT) activity, using the method of O'Brien (*37*) and the pyrophosphate reagent from Sigma (cat. no. P7275), which couples the production of pyrophosphate to the consumption of NADH. For this assay, *P*PAT from *E. coli* (EcCoaD) was used, prepared as previously described (*38*). Each 500 μL assay mixture contained 200 μL of pyrophosphate reagent, 0.5 mM *P*PC (**1**), 2.0 mM ATP, 1.0 mM DTT, 10 mM $MgCl_2$, 20 mM KCl, 15 μg of 6×His-EcCoaD (∼1.5 μM final), and 0.75 μg of 6×His-HsCoaC (∼60 nM final) in 50 mM Tris-HCl buffer (pH 7.6). The reaction was initiated by addition of substrate **1** and mixed by inversion, and the decrease of NADH concentration was monitored by changes in absorbance at 340 nm.

For time-dependent inhibition assays, a 100 μL inhibition mixture containing *P*PanΔSH (**3**) (0.5−6.0 mM), 10 mM DTT, 10 mM $MgCl_2$, and 150 μg of 6×His-HsCoaC (∼60 μM final) in 50 mM Tris-HCl buffer (pH 8.0) was incubated at 37 °C. Periodically, 10 μL aliquots were removed and diluted to 1.0 mL, and 50 μL of the diluted solution was used to replace the 6×His-HsCoaC in the assay mixture (giving a final 6×His-HsCoaC concentration of ∼60 nM). The amount of remaining activity was then determined as described above.

For substrate protection assays, the inhibition mixtures also contained *P*PC (**1**) (0.3−5.0 mM), while the concentration of inhibitor *P*PanΔSH (**3**) was kept constant at 3.0 mM.

Data Analysis. Data were analyzed using Origin 6.0 (Microcal) and were fit to the Michaelis−Menten equation (K_m and k_{cat} determinations) or to eq 1,

$$y = y_0 + A\,e^{-kt} \quad (1)$$

for the inhibition studies, with $y_0 + A = 100$ to obtain percent remaining activity. For the time-dependent inhibition studies of *P*PC-DC, the value of *A* was set to 100, while the data from the substrate protection experiment were analyzed with *A* and y_0 set as variables to obtain the limiting values for the extent of inhibition.

Flavin Absorption Spectra. Flavin spectra were measured at 25 °C using 500 μL reaction mixtures containing either 5.0 mM *P*PC (**1**), 5.0 mM *P*PantSH (**2**), or 5.0 mM *P*PanΔSH (**3**) and 5 mM DTT, 10 mM $MgCl_2$, and 1.0 mg of 6×His-HsCoaC (∼80 μM final) in 50 mM Tris-HCl buffer (pH 8.0). Spectra of the mutant enzyme 6×His-CoaC C173S were measured in a similar fashion using 1.0 mg of protein in a 500 μL reaction mixture. Spectra of 6×His-CoaC C173S were also measured in the presence of 4′-phosphopantothenate (**30**).

Sample Preparation for FTMS Analysis. FTMS analysis of labeled protein was performed on reaction mixtures containing rTEV-treated HsCoaC (100 μg), 5 mM *P*PanΔSH (**3**), 10 mM DTT, and 10 mM $MgCl_2$ in 50 mM Tris-HCl (pH 8.0) in a total volume of 50 μL. Label localization was achieved after proteolysis of enzyme treated with the inhibitor **3**. Reaction mixtures contained 6×His-HsCoaC (230 μg), 6 mM *P*PanΔSH (**3**), 10 mM DTT, and 10 mM $MgCl_2$ in 50 mM Tris-HCl (pH 8.0) in a total volume of 150 μL. Mixtures were incubated for 2 h at 37 °C followed by buffer exchange to 10 mM Tris-HCl (pH 7.4) using Micro Bio-spin 6 gel filtration columns (Biorad) prior to protease treatment.

*Proteolysis. P*PanΔSH-treated 6×His-HsCoaC was denatured with 4 M guanidinium hydrochloride chloride or 1 M urea prior to proteolysis with either Lys-C (1 μg per 40 μg of treated protein) or Glu-C (1 μg per 100 μg of treated protein) in 20 mM Tris-HCl (pH 7.8) at 37 °C for 2−18 h. Guanidine was removed prior to digestion by buffer exchange, while digestion was performed in the presence of

Scheme 5 [a]

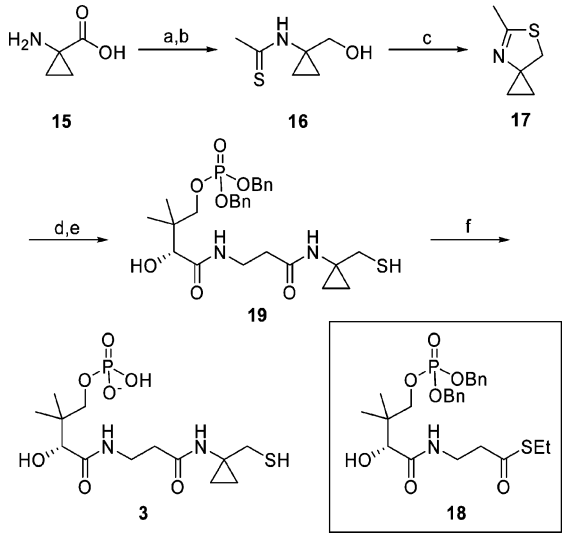

[a] Reagents and conditions: (a) BH_3, THF; (b) ethyldithioacetate, DIPEA, MeOH; (c) [bis(2-methoxyethyl)amino]sulfur trifluoride (Deoxo-Fluor), CH_2Cl_2, −20 °C; (d) 2.5 M HCl, reflux; (e) **18**, DIPEA, MeOH; (f) Na/liq NH_3.

urea. The reaction mixtures were quenched by the addition of 5 μL of acetic acid prior to analysis.

FTMS Analysis. All samples were desalted by loading onto a reverse-phase peptide trap (Michrom Bioresources, Auburn, CA). The trap was washed with 2 mL of H_2O/MeOH/AcOH (98:1:1) and eluted with 80 μL of H_2O/MeOH/AcOH (20:76:4). The solutions were electrosprayed at 1−50 nL/min with a nanospray emitter (*39*). The resulting ions were guided through a heated metal capillary, a skimmer, and three radio frequency-only quadrupoles into a 6 T Finnigan FTMS with the Odyssey data system (*40*). The outer trapping electrodes, conventionally used for electron containment, are used for ion trapping. Assignments of the fragment masses and compositions were made with the computer program THRASH (*41*). The mass difference (in units of 1.002 35 Da) between the most abundant isotopic peak and the monoisotopic peak is denoted in italics after each M_r value.

ESI-MS Analysis. All enzymatic reaction mixtures submitted for ESI-MS analysis were treated as follows prior to injection: Reaction mixtures were loaded on a Dowex 50WX8-100 column (500 μL) equilibrated in deionized water, and the column was eluted with 2 × 500 μL of deionized water. The eluate was lyophilized, and resuspended in a solution of 50% aqueous acetonitrile. Reaction mixtures contained 5 mM substrate (*P*PC (**1**)) or *P*PanΔSH (**3**)**)**, 6×His-HsCoaC (270 μg) or 6×His-HsCoaC C173S (1 mg), 5 mM DTT, and 10 mM $MgCl_2$ in 50 mM Tris-HCl (pH 8.0) in a total volume of 150 μL. Mixtures were incubated for between 22 and 48 h before Dowex treatment.

RESULTS

Synthesis of PPanΔSH. The proposed inhibitor **3** was synthesized as shown in Scheme 5. The synthesis used ACC (**15**) as the source of the cyclopropyl group and is based on borane-mediated reduction of the carboxylic acid of **15** to the alcohol, followed by conversion of the alcohol to the thiol via the thiazolidine intermediate **17**. Hydrolysis gives (1-amino-cyclopropyl)-methanethiol, which can easily react with the thioester **18** in a transthioesterification reaction. Finally the product **19**, which forms after rearrangement to the more stable amide, is deprotected to give *P*PanΔSH (**3**).

Theoretical Analysis of the Inhibition of PPC-DC by PPanΔSH (3). The use of *P*PanΔSH (**3**) as an electrophilic trap of active site nucleophiles (such as B_2H/B_2^- shown in Scheme 2) requires activation by oxidation of the thiol group to a thioaldehyde, as shown in Scheme 6. *P*PanΔSH (**3**) can react with the enzyme in three ways. In pathway a, ring opening of **22** by B_2^- or B_2H would give the enethiolate **23** and reduced flavin, which can be oxidized by solvent-dissolved oxygen to give **24**. If the inactivating agent **3** does not label the active site acid involved in enethiolate protonation, then **23** could tautomerize to **27** as shown for pathway b. Reduction of the thioaldehyde of **27** would give **28**. In pathway c, thioaldehyde **22** is released from the enzyme and hydrolyzed to give **29**. It should be possible to differentiate experimentally among these three pathways. Adducts **24** and **28** are expected to show different charge-transfer absorption bands and can be identified by mass spectrometry because they differ by two mass units. In addition, **24** could undergo slow hydrolysis to **26**, while such hydrolysis is not possible for **28**. If the reaction occurs via pathway c, it should be possible to detect **29** in the small molecule pool. In all cases, the enethiol tautomers are shown to be preferentially formed in agreement with both experimental and theoretical studies on tautomerism in thiocarbonyl systems (*42*−*44*).

PPanΔSH as a Substrate for PPC-DC. *P*PC-DC was treated with **3** for a period of 48 h, followed by ESI-MS analysis of the small molecules in the reaction mixture. Only unmodified FMN and unreacted *P*PanΔSH (**3**) could be detected (Figure 1). This argues against the formation of the turnover products **22** and **29** by pathway c.

Flavin Is Not Modified by PPanΔSH (3). Reaction mixtures containing *P*PC-DC incubated with substrate *P*PC (**1**) and the inhibitor *P*PanΔSH (**3**) were analyzed for the presence of flavin adducts by ESI-MS. In both cases, the reaction mixtures were gel-filtered to remove unreacted small molecule components and were then acidified prior to analysis. Only unmodified FMN was detected in both samples; no compounds with the expected molecular weight of a flavin−*P*PanΔSH adduct could be detected (results not shown), demonstrating that *P*PanΔSH (**3**) does not form stable reaction products with the flavin cofactor at detectable levels.

Inactivation of PPC-DC by PPanΔSH: Kinetic Analysis. The effect of *P*PanΔSH (**3**) on the *P*PC-DC activity was tested by incubating the enzyme with **3** at 37 °C, pH 7.6, removing aliquots of protein at set time intervals, and determining the amount of remaining activity after 100-fold dilution. This was repeated at increasing concentrations of *P*PanΔSH. The results, summarized in Figure 2, show that compared to a control sample *P*PanΔSH (**3**) inactivates the enzyme in a time-dependent fashion, higher concentrations achieving this inactivation faster. The results also show that at later time points the inhibition exhibits non-pseudo-first-order kinetics, especially in the case of higher concentrations of inhibitor. This may happen if a product of the reaction accumulates in the reaction mixture and protects the protein against inactivation by competing with the inhibitor. However, since no turnover products could be detected in reaction mixtures by ESI-MS analysis, the enzyme protection must

Scheme 6

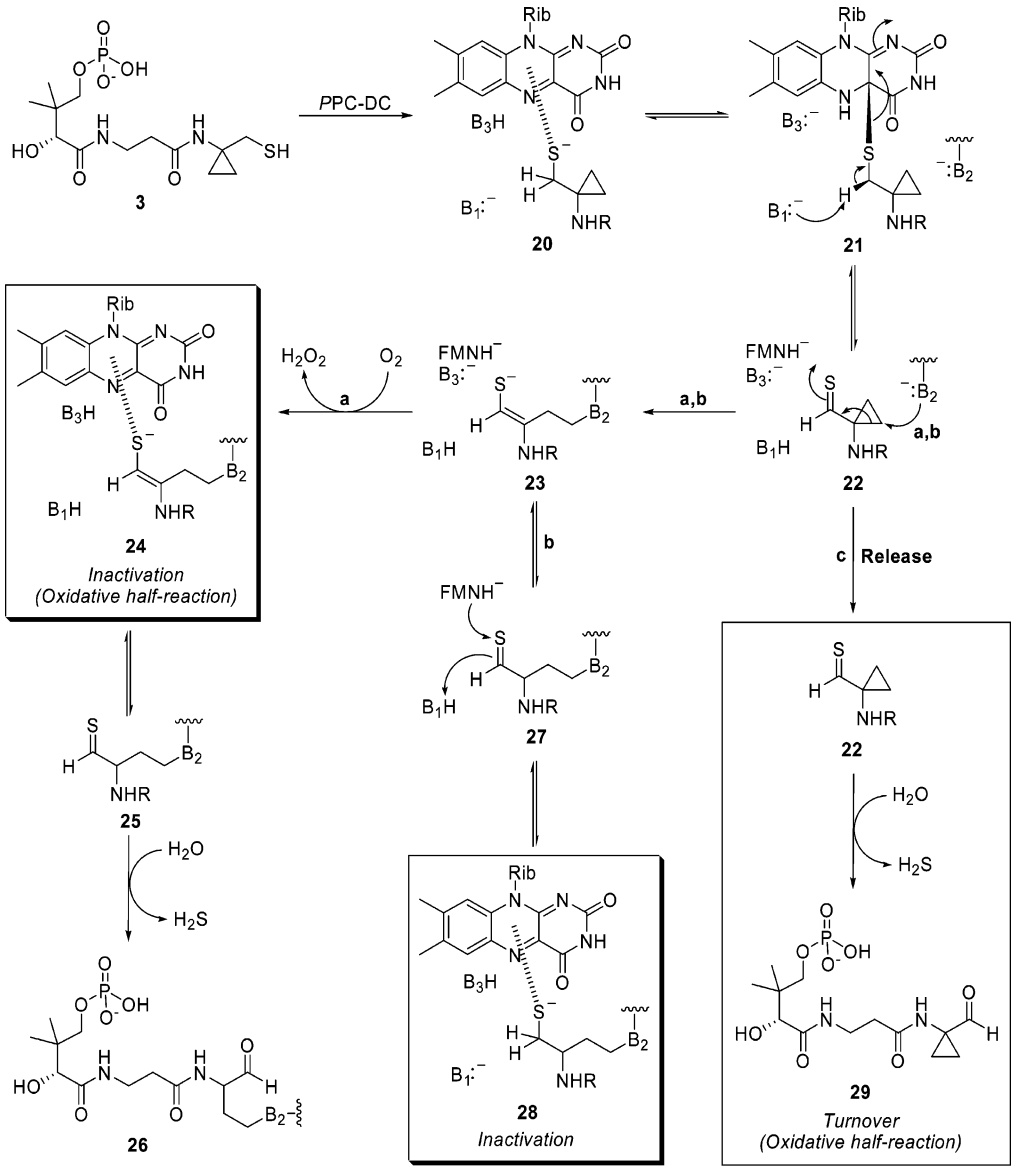

be due to some other phenomenon. Our previous studies on the bifunctional protein from *E. coli*, which is a native dodecamer, suggested that *P*PC-DC activity is regulated by allosteric interactions or cooperative effects (*36*). It is likely that a similar situation holds for the human enzyme used in this study, a native trimer (*45*), where inactivation at one active site influences activity at an adjacent site and consequently results in a diminished rate of inactivation. Since the inhibitor *P*PanΔSH (**3**) is structurally similar to product, it can also mimic any possible regulatory effects normally mediated by the product in an allosteric manner.

Having demonstrated saturation kinetics for the inhibition of the enzyme, we determined the K_I and k_{inact} values for *P*PanΔSH (**3**) by plotting the half-life for inactivation, as calculated from the data in Figure 2, against the reciprocal of the inhibitor concentration (Kitz−Wilson plot) (*46*). The resulting linear plot ($R^2 = 0.99$) gave values for K_I of 2.58 ± 0.13 mM and k_{inact} of 0.15 ± 0.01 min^{-1}, compared to the K_m of 118.5 ± 17.1 μM and k_{cat} of 2.9 ± 0.1 s^{-1} values determined using the substrate *P*PC (**1**).

To show that inactivation is occurring at the active site of the protein, *P*PC-DC was treated with 3.0 mM *P*PanΔSH as before but in the presence of increasing concentrations of substrate **1**. The results indicate the time-dependent inactivation of the enzyme, as shown in Figure 3. However, the presence of substrate protects the enzyme against inactivation, leading to a decrease in the rate of activity loss. Furthermore, loss of activity did not proceed beyond a certain level, which is dependent on substrate concentration. The mechanistic implications of this behavior are not clear at this point but support the proposed ability of the substrate **1** or product **2** to regulate enzyme activity by cooperative binding effects between the various active sites of the native trimeric protein.

Detecting Stable Protein−PPanΔSH Adducts by FTMS. Since the kinetic studies demonstrated that *P*PanΔSH (**3**) acts as a mechanism-based inhibitor of *P*PC-DC, we set out to identify and characterize the protein adduct by FTMS. Initial results using the recombinant 6×His-CoaC protein indicated mass heterogeneity due to the removal of some amino acid residues from the N-terminus. To address this problem, the protein was treated with rTEV protease, which selectively removes the 6×His-tag. Protein treated in this way gave homogeneous mass spectra with high mass

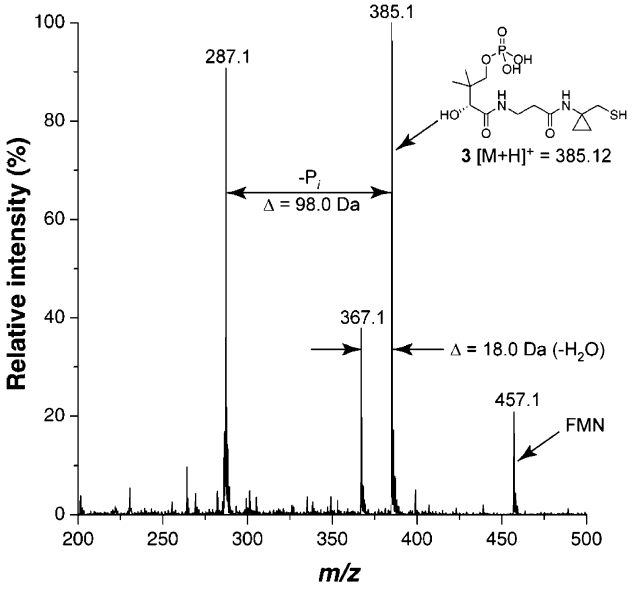

FIGURE 1: ESI-MS analysis (positive mode) of a reaction mixture of human *P*PC-DC and *P*PanΔSH (**3**) incubated for a period of 48 h at 37 °C, showing the presence of only unreacted **3** and the flavin cofactor. Other peaks are the result of the fragmentation the molecular ion ($[M + H]^+$) of **3**, leading to loss of either phosphate or water as indicated by the mass differences.

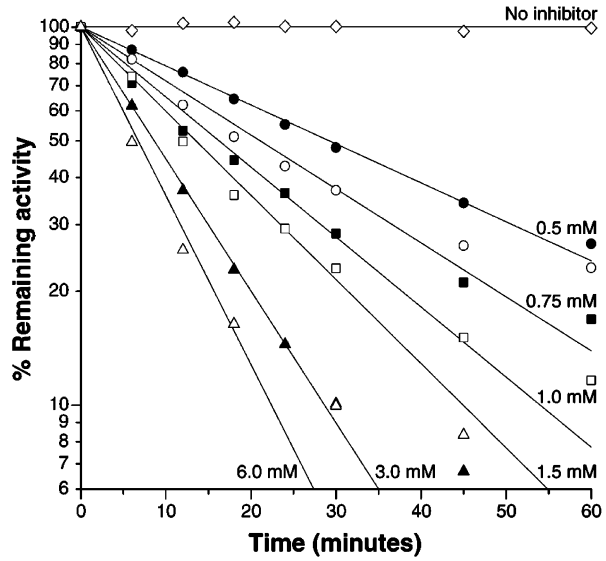

FIGURE 2: Time-dependent inactivation of *P*PC-DC by increasing concentrations of *P*PanΔSH (**3**), showing saturation of inhibition at higher concentrations. Reactions were performed at 37 °C at pH 7.6. The solid lines indicate the best fit of the data to an equation for exponential decay to zero (see Experimental Procedures for details).

precision, as shown in Figure 4A. Subsequently, a reaction mixture of *P*PC-DC incubated with the inhibitor *P*PanΔSH (**3**) was analyzed in a similar fashion for the presence of a *P*PanΔSH-derived protein adduct, which should add 382.0 Da to the mass of rTEV-treated 6×His-HsCoaC. The results are summarized in Figure 4B. Treated protein exhibited peaks in the mass spectra corresponding to both unlabeled protein and protein with either a 382.2 or 366.1 Da mass addition as shown. When the mass spectrum of the same sample was taken 6 h later the intensity of the 366.1 Da adduct had increased at the cost of the 382.2 Da adduct, indicating the decomposition of the latter to form the more stable derivative with −16 Da mass difference. These results are in agreement

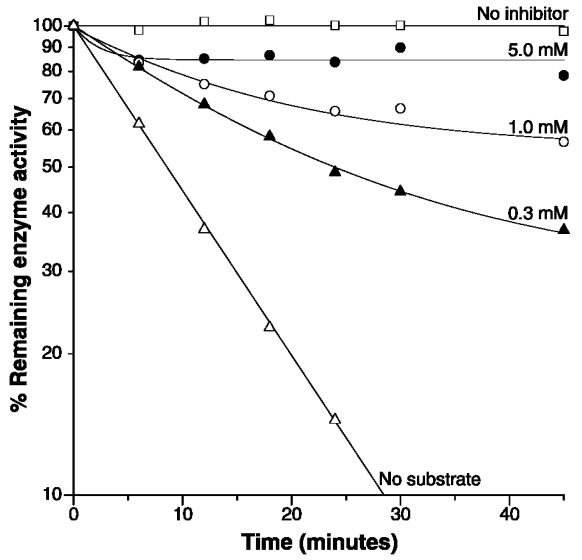

FIGURE 3: Substrate protection of *P*PC-DC against inactivation by 3.0 mM *P*PanΔSH. Reactions were performed at 37 °C at pH 7.6. The solid lines indicate the best fit of the data to an equation for exponential decay to a set value (see Experimental Procedures for details).

with the formation of a covalent *P*PanΔSH-derived protein-adduct complex **24** by pathway a (Scheme 6), since hydrolysis of **24** will result in the exchange of sulfur for oxygen (S − O = 16 Da). Formation of the reduced complex **28** by pathway b can be excluded because mass accuracy in FTMS is within 1 Da, allowing it to distinguish between **24** and **28**, which differ by 2 Da units in mass. In addition, the reduced adduct **28** should be stable to hydrolysis.

Localization of the Site of Modification of PPC-DC. To determine which amino acid was modified upon reaction of *P*PanΔSH (**3**) with *P*PC-DC, the enzyme was incubated with the inhibitor and treated separately with Lys-C and Glu-C endoproteinases. After overnight incubation, the resulting peptide mixtures were analyzed by FTMS. The resulting spectra showed peaks corresponding to the masses of nearly every expected peptide, as well as some peptides resulting from partial proteolysis, as shown in Tables 1 and 2. Both the Lys-C and Glu-C digests also show a ∼366.1 Da mass adduct on peptides from the same region of the protein, corresponding to a covalent adduct. The sequences of two of the peptides that carry this mass adduct are represented on the sequence of the protein in Figure 5 and show that the sequence ^{170}KLVCGDE^{176} is present in both of these peptides. This analysis leads to the identification of an amino residue contained in the sequence ^{170}KLVCGDE^{176} as the site of covalent modification.

Native PPC-DC Thiolate−Flavin Charge-Transfer Complexes. Our previous mechanistic studies on *P*PC-DC from *E. coli* showed the presence of substrate- and product-induced thiolate−flavin charge-transfer complexes (*4*). The native human enzyme also forms a charge-transfer complex in the presence of *P*PC (**1**) (Figure 6A). Over time the initial charge-transfer band (absorbance maximum of ∼580 nm) undergoes a red shift (absorbance maximum of ∼690 nm) and diminishes in intensity. The enzyme interacts with the product **2** in a similar way, although the intensities of the charge-transfer absorptions are lower (Figure 6B). These observations are consistent with the conversion of the initial

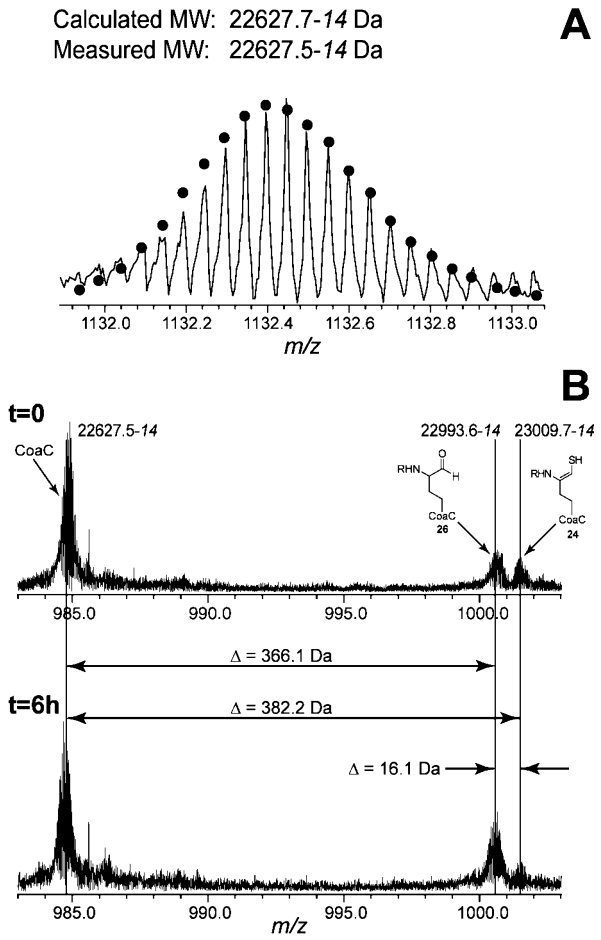

FIGURE 4: FTMS analysis of *P*PC-DC inactivation: (A) mass spectrum of the 6×His-HsCoaC protein treated with rTEV protease to remove the N-terminal His-tag fusion; (B) mass spectra of a sample of the protein treated with *P*PanΔSH (**3**) immediately after incubation and removal of the inhibitor ($t = 0$) and of the same sample 6 h later ($t = 6$ h), showing that the protein is covalently labeled, as indicated by the presence of additional peaks, and that the heavier species (**24**) converts to the lighter species (**26**) over time in the acidic buffer used for MS analysis.

Table 1: Peptide Fragments Resulting from Lys-C Endoprotease Digestion of Recombinant Human *P*PC-DC Treated with *P*PanΔSH (**3**)

mass[a]	assignment[b]	error (Da)[c]	mass[a]	assignment[b]	error (Da)[c]
718.34, *0*	$G^{-2}-K^{4}$	+0.04	13989.1, *8*	$S^{81}-S^{204}$	+366.0
1343.75, *0*	$A^{5}-K^{17}$	+0.08	2338.21, *1*	$V^{111}-K^{131}$	+0.07
1496.95, *0*	$F^{18}-K^{32}$	+0.07	2982.55, *1*	$P^{132}-K^{157}$	+0.08
768.56, *1*	$L^{33}-K^{39}$	+0.04	1295.73, *0*	$A^{158}-K^{169}$	+0.07
1924.14, *1*	$L^{40}-K^{57}$	+0.02	1423.84, *0*	$A^{158}-K^{170}$	+0.08
2857.40, *1*	$H^{58}-K^{80}$	+0.04	2698.40, *1*	**$K^{170}-K^{192}$** [d]	+366.02
10048.14, *6*	$S^{81}-K^{170}$	+0.05	1405.73, *0*	$E^{193}-S^{204}$	+0.07

[a] The mass difference (in units of 1.002 35 Da) between the most abundant isotopic peak and the monoisotopic peak of peptide fragments is denoted in italics after each M_r value. [b] Assigment based on known protein sequence and determined mass. [c] Error based on comparison of measured and calculated mass of assigned peptide. [d] Fragment highlighted in Figure 5.

thiolate−flavin charge-transfer complex to a charge-transfer complex with the enethiolate **7** in both cases; the enethiolate−flavin charge-transfer complex subsequently slowly decomposes due to enzyme instability or due to nonenzymatic oxidation of the substrate and product thiol. In contrast, when the enzyme is treated with *P*PanΔSH (**3**), the initially

Table 2: Peptide Fragments Resulting from Glu-C Endoprotease Digestion of Recombinant Human *P*PC-DC Treated with *P*PanΔSH (**3**)

mass[a]	assignment[b]	error (Da)[c]	mass[a]	assignment[b]	error (Da)[c]
1158.54, *0*	$N^{-7}-E^{2}$	+0.03	2044.09, *1*	$H^{146}-E^{163}$	+0.05
23292.3, *14*	$N^{-7}-S^{204}$	+366.7	1739.82, *0*	**$I^{164}-E^{176}$** [d]	+366.10
717.40, *0*	$V^{48}-E^{54}$	+0.01	1086.65, *0*	$V^{184}-E^{193}$	+0.02
11177.98, *7*	$V^{48}-E^{145}$	+0.04	2346.26, *1*	$V^{184}-S^{204}$	+0.02
2767.38, *1*	$R^{55}-E^{77}$	+0.08	1276.67, *0*	$V^{184}-S^{204}$	+0.05

[a] The mass difference (in units of 1.002 35 Da) between the most abundant isotopic peak and the monoisotopic peak of peptide fragments is denoted in italics after each M_r value. [b] Assigment based on known protein sequence and determined mass. [c] Error based on comparison of measured and calculated mass of assigned peptide. [d] Fragment highlighted in Figure 5.

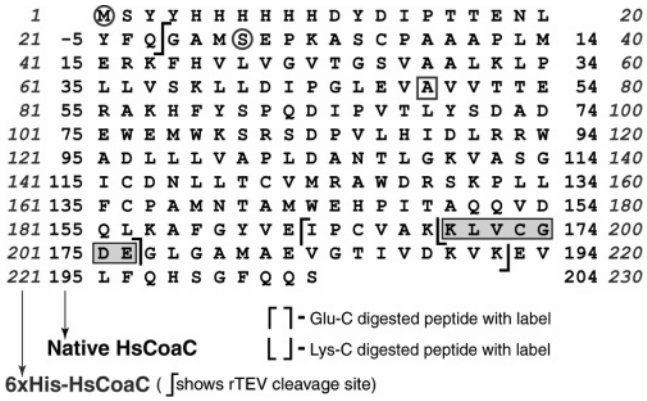

FIGURE 5: Sequence of the recombinant *P*PC-DC (6×His-HsCoaC) showing the Lys-C and Glu-C peptide fragments containing the 366 Da mass adduct. The sequence spanned by both fragments is contained in the shaded box. Tandem mass spectrometry identified the boxed alanine previously assigned as a serine. Sequence numbering is for the 6×His-CoaC fusion protein (italics) and the native enzyme (bold), each starting with the indicated circled residues. The latter numbering system is used throughout the paper.

formed charge-transfer complex is rapidly converted into a species with the same absorption as the putative enethiolate−flavin (Figure 6C). This species is stable and is present in higher concentrations than the corresponding complexes with substrate and product as expected for an enethiolate that is covalently linked to the protein. This result supports the formation of the enethiolate−flavin complex **24** (Scheme 6).

PPC-DC (C173S) Thiolate−Flavin Charge-Transfer Complexes. The mutant human *P*PC-DC in which Cys^{173} has been changed to serine was prepared by site-directed mutagenesis, followed by expression and purification as a stable green protein. Its UV−visible spectrum shows a long wavelength absorption that is similar to that of the putative enethiolate−flavin charge-transfer complexes induced by **1**, **2**, and **3** in native *P*PC-DC (Figures 6 and 7). The stable green complex reverts to the normal yellow color of the native enzyme upon treatment with the substrate analogue 4′-phosphopantothenate (**30**) (Figure 7, trace 3). This suggests that the C173S mutant contains the tightly bound enethiolate intermediate **7**, which can be displaced by **30**.

The time-dependent changes in the flavin absorption spectrum of the mutant enzyme in the presence of substrate *P*PC (**1**), product *P*PantSH (**2**), and inhibitor *P*PanΔSH (**3**) are shown in Figure 8. Since the enethiolate **7** copurifies with the mutant protein and could not be removed by simple

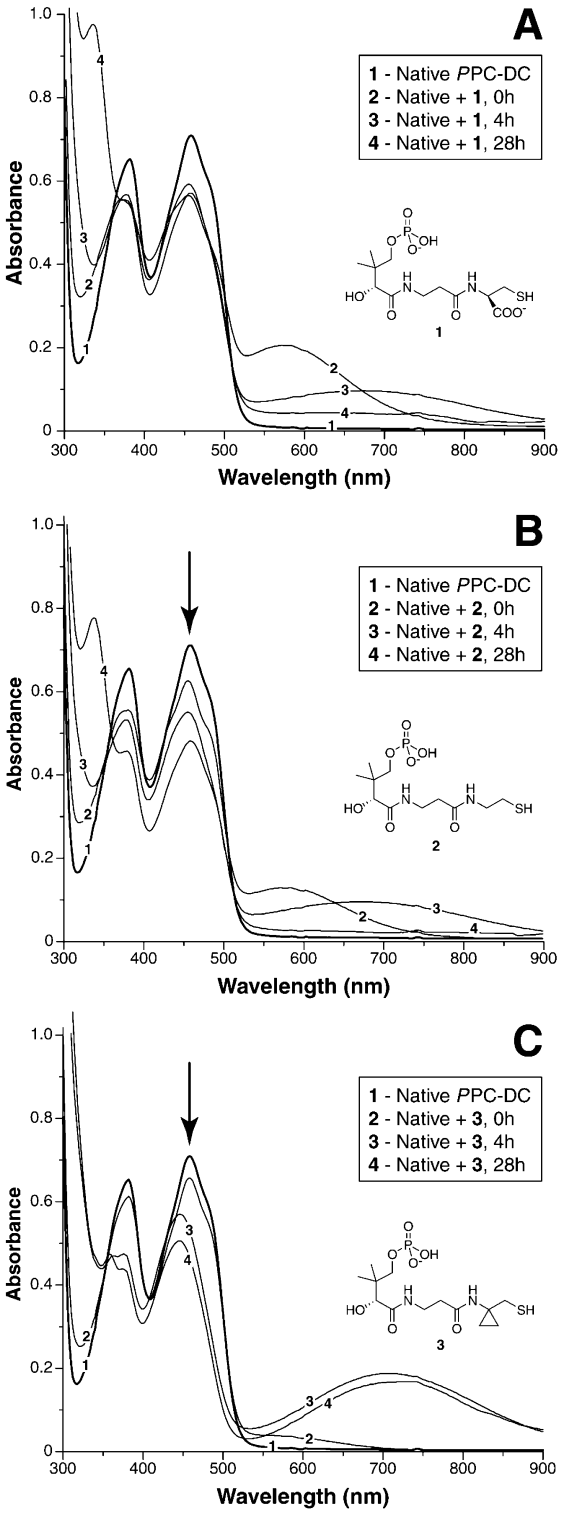

FIGURE 6: Time-dependent changes in the flavin absorption spectrum of human *P*PC-DC in the presence of (A) *P*PC (**1**), the natural substrate of *P*PC-DC, (B) *P*PantSH (**2**), the product of the reaction, and (C) the mechanism-based inactivator *P*PanΔSH (**3**) under aerobic conditions. In each case, compounds **1**, **2**, and **3** are present at a final concentration of 5.0 mM, at pH 8.0. The untreated protein (line 1) is shown in bold.

gel filtration, samples also contained small amounts of this compound, as evidenced by the absorption exhibited at 690 nm by the untreated protein (Figure 8A,B,C, trace 1). However, since sufficient amounts of substrate, product, or inhibitor (5.0 mM, compared to ~80 μM enzyme) were added to displace **7** from the active site, its affect on the

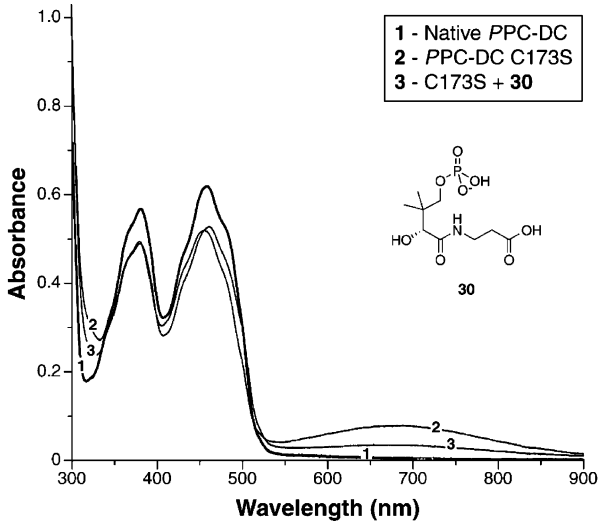

FIGURE 7: Flavin absorption spectra of the native *P*PC-DC (line 1, bold) and the *P*PC-DC C173S mutant (line 2). The mutant enzyme shows the presence of a stable long-wavelength absorption, which disappears when the substrate analogue **30** (4′-phosphopantothenate) is added (line 3).

other absorption spectra shown in Figure 8 was considered to be small. When treated with substrate **1**, the flavin cofactor is reduced and is slowly reoxidized, presumably by solvent-dissolved oxygen, regenerating the enethiolate−flavin charge-transfer complex (Figure 8A). The very slow rate of this reoxidation reaction is consistent with the protein providing the reduced flavin cofactor with the necessary protection from solvent to allow reduction of the thioaldehyde in the normal catalytic reaction.

Treatment of the mutant protein with *P*PantSH (**2**) (Figure 8B) results in the formation of an initial absorption at 580 nm similar to that seen in the spectra of the native enzyme treated with either substrate or product (Figure 6A,B); however, in the case of the mutant enzyme, this absorption does not undergo a red shift and no absorption at 690 nm is formed. This shows that, unlike the native enzyme, the mutant protein cannot convert the product *P*PantSH (**2**) into the enethiol **7**. Finally, the presence of the inhibitor **3** fails to have any extensive effect on the absorption spectrum of the protein, indicating that the inhibitor does not undergo oxidation or ring opening in the active site of the mutant enzyme (Figure 8C).

PPC as a Substrate for the PPC-DC C173S Mutant. When a reaction mixture containing the mutant enzyme and the substrate *P*PC (**1**) was analyzed by ESI-MS, the resulting spectrum showed the presence of new peaks. One of these corresponded to the mass of the enethiolate intermediate **7**, and another matched the mass of its hydrolysis product, the aldehyde **31** (Figure 9). This demonstrates that the mutant protein is incapable of reducing **7** and supports the assignment of the charge-transfer complex of the purified mutant protein to the interaction of flavin with the enethiolate **7**.

DISCUSSION

The *P*PC-DC-catalyzed decarboxylation of *P*PC (**1**) proceeds by initial flavin-mediated oxidation of *P*PC to the thioaldehyde **6** followed by decarboxylation to give the enethiolate **7**. Protonation followed by reduction completes the reaction (Scheme 2). In contrast to *P*PC-DC, the

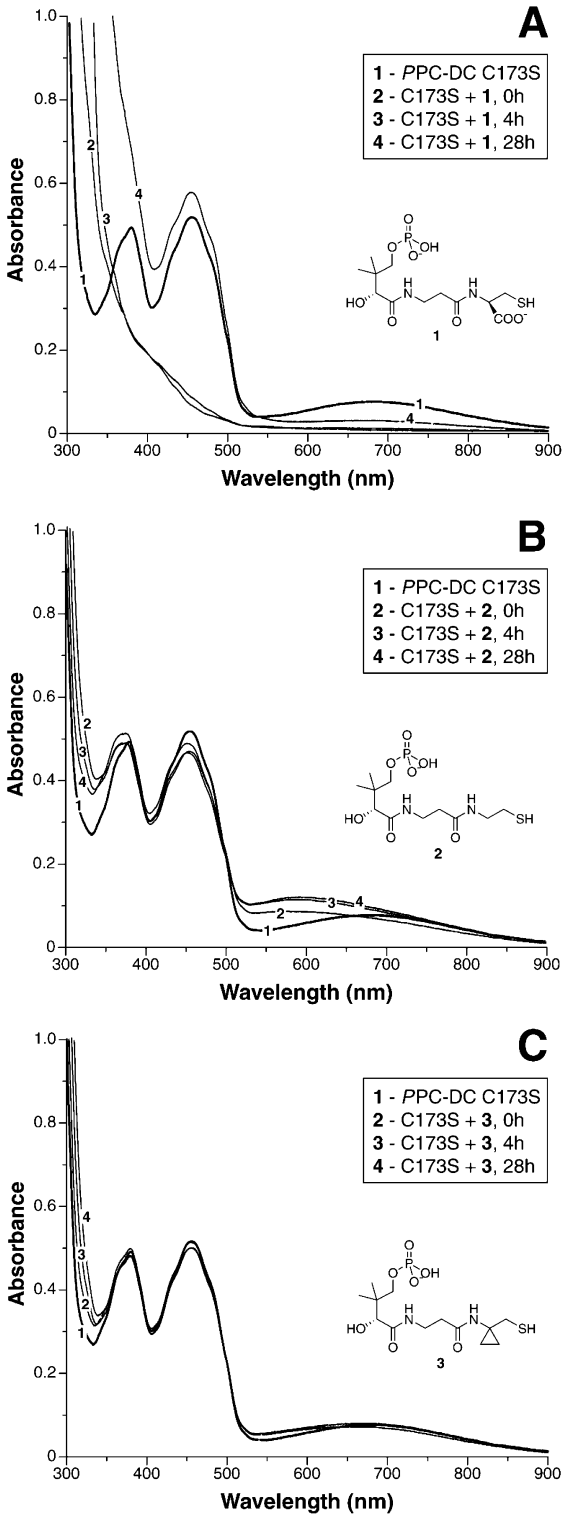

FIGURE 8: Time-dependent changes in the flavin absorption spectrum of the C173S mutant human *P*PC-DC in the presence of (A) *P*PC (**1**), the natural substrate, (B) *P*PantSH (**2**), the product of the reaction, and (C) the mechanism-based inactivator *P*PanΔSH (**3**) under aerobic conditions. In each case, compounds **1**, **2**, and **3** are present at a final concentration of 5.0 mM, at pH 8.0. The untreated protein (line 1) is shown in bold.

flavoenzymes EpiD and MrsD catalyze the decarboxylation of a peptidyl-cysteine moiety, but the reaction does not proceed beyond the enethiol for these enzymes (Scheme 3). In this paper, we address the mechanistic basis for the different catalytic activities of these two closely related members in the family of cysteine decarboxylases.

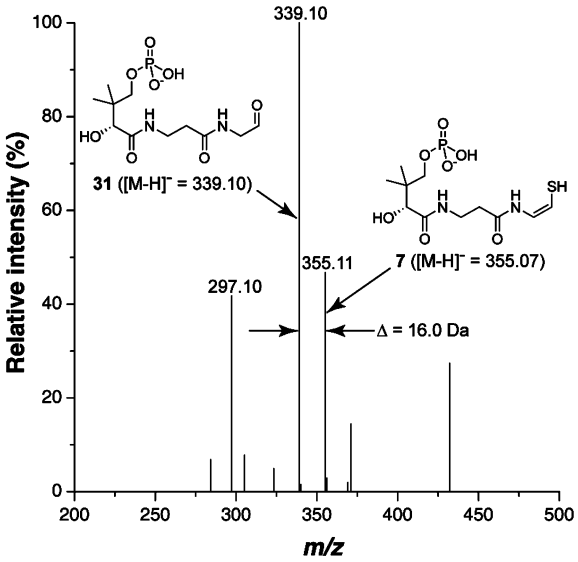

FIGURE 9: ESI-MS analysis (negative mode) of a reaction mixture of the C173S mutant of *P*PC-DC and substrate *P*PC (**1**) incubated for a period of 22 h at 37 °C. In comparison to a control sample without substrate, the mass spectrum shows new peaks, which are labeled. These correspond to the molecular ions ($[M - H]^-$) of the enethiolate **7** and its hydrolysis product, the aldehyde **31**.

Both experimental and theoretical studies have shown that in contrast to the oxygen system the tautomeric equilibrium established between an enethiol and its thiocarbonyl tautomer usually favors the enethiol (*42*, *43*). Furthermore, the enethiol product (rather than the corresponding thioaldehyde) has been directly observed in the EpiD system by ^{13}C NMR spectroscopy (*44*) and has been shown to have a pK_a of ~6.0 (*34*). However, the mechanism outlined for *P*PC-DC in Scheme 2 requires that the enethiolate intermediate be protonated to form the thioaldehyde before reduction can occur. This protonation can be accomplished by an active site acid.

On the basis of this analysis, we proposed that the key difference between the simple decarboxylation catalyzed by *P*PC-DC and the oxidative decarboxylation catalyzed by both EpiD and MrsD is the presence of an active site acid capable of protonating the enethiolate **7**. In the presence of this acid, enethiolate **7** is protonated to give thioaldehyde **8**, which can subsequently be reduced by the dihydroflavin to give net decarboxylation of the substrate without a change in its oxidation state. This reduction cannot occur in the absence of the protonation step, and the reaction therefore stops at the enethiolate as observed in the oxidative decarboxylation reactions. This hypothesis is supported by the presence of an active site cysteine residue in *P*PC-DC, which is exchanged for serine and threonine (both weaker acids) in EpiD and MrsD, respectively (*12*, *15*, *17*). Furthermore, when the active site cysteine (Cys^{175}) of the *A. thaliana P*PC-DC (AtHAL3a) was replaced by serine, the resulting mutant protein became an oxidative decarboxylase (*14*). These observations strongly suggested that the active site cysteine in *P*PC-DC protonates the enethiol intermediate at C_α (the carbon adjacent to the amide nitrogen). However, the crystal structure of the *A. thaliana P*PC-DC C175S mutant with the dephosphorylated enethiolate (dephospho-**7**) bound at the active site demonstrates that the thiol of Cys^{175} is too far (4.17 Å) from the α-carbon of the enethiolate for optimal proton transfer (*18*). In addition, several other mutants of *A.*

*thaliana P*PC-DC gave mixtures of enethiol and pantetheine products, casting doubt on the hypothesis that a single residue is responsible for controlling the differing catalytic activities. To remove this ambiguity, we have synthesized a substrate analogue (*P*PanΔSH (**3**)) designed to alkylate the putative active site acid. If our mechanistic analysis is correct, such an alkylation would result in the trapping of the enethiolate intermediate by preventing its protonation.

We find that *P*PanΔSH (**3**) is a mechanism-based inhibitor of human *P*PC-DC. The inhibition is time-dependent and shows saturation kinetics. In addition, substrate **1** protects the enzyme from inactivation, demonstrating that the inactivation occurs at the active site (Figures 2 and 3). MS analysis of the inactive enzyme demonstrates that *P*PanΔSH (**3**) alkylates the protein rather than the flavin cofactor (Figures 1 and 4B). Inactivation is also very efficient because ESI-MS analysis of the small molecules in the inactivation reaction mixture fails to detect turnover products derived from **3**.

ESI-FTMS analysis of the labeled enzyme demonstrated the formation of two adducts, one with a mass corresponding to **23** and the other with a mass corresponding to **26**, the hydrolysis product of **23** (Figure 4 and Scheme 6). Compound **23** is likely to be formed by oxidation of **3** to **22**, which then alkylates the enzyme. Oxidation of **23** to **24** followed by slow hydrolysis would give **26** (Scheme 6, pathway a). The observed mass of the alkylated protein, as well as the detection of the hydrolysis product **26**, is not consistent with the formation of **28** because the mass of **28** is 2 Da heavier than the mass of **24** and the sulfur on **28** cannot be removed by hydrolysis. Failure to form **28** suggests that **22** alkylates the active site acid involved in enethiolate protonation. The formation of **24** is also supported by the observation of a stable thiolate−flavin charge-transfer absorption at 690 nm, which is different from the enzyme−substrate and enzyme−product charge-transfer complexes, which both absorb at 590 nm (Figure 6).

The site of alkylation was localized to the ^{170}KLVCGDE^{176} peptide by ESI-FTMS analysis of LysC and GluC proteolysis mixtures (Figure 5). Four amino acids in this sequence are possible nucleophiles in the ring-opening reaction of *P*PanΔSH: Lys^{170}, Cys^{173}, Asp^{175}, and Glu^{176}. Lys^{170} and Glu^{176} can be excluded as candidates since these residues were still recognized by LysC and GluC during the proteolysis. Ring opening by Asp^{175} would lead to the formation of a labile ester linkage between *P*PanΔSH and the protein but is unlikely since the labeled peptide is stable during the proteolysis under conditions that should result in ester hydrolysis (2−18 h at pH 7.8). This suggests that Cys^{173}, which is equivalent to the active site Cys^{175} of the *A. thaliana P*PC-DC (*14*, *18*), is the alkylated residue.

FTMS analysis of fully inactivated enzyme demonstrated that only about a third of the protein was modified by **3** (Figure 4B). We considered two possible explanations for this observation. First, low amounts of labeled protein could result from hydrolysis of a labile linkage such as an ester. However, the observed stability of the adduct would argue against the likely occurrence of such an event. A second and more probable explanation for the low labeling efficiency is that labeling at the active site of one subunit of the trimeric HsCoaC protein renders the other subunits catalytically inactive and therefore incapable of being labeled. This explanation is also consistent with the rate of inactivation deviating from first-order kinetics at later time intervals and at high concentration of inhibitor, as seen in Figures 2 and 3.

The properties of the C173S mutant of *P*PC-DC were consistent with Cys^{173} functioning as the active site acid involved in enethiolate protonation. The mutant was unable to catalyze the reduction of the enethiolate intermediate formed from **1** and was isolated as a stable complex with the enethiolate showing an absorption spectrum similar to that of the inactivated enzyme (Figures 6C and 7). This enethiolate was also characterized by mass spectrometry and could be displaced from the active site using the substrate analogue **30**. Treatment of the mutant enzyme−enethiolate complex with substrate **1** resulted in the rapid bleaching of the charge-transfer complex followed by its slow return after prolonged incubation. This observation is in agreement with the oxidative decarboxylation of the substrate to the enethiolate/dihydroflavin complex. The complex is stable and shows only slight reoxidation after 28 h. This stability is consistent with our previous observation that the *E. coli P*PC-DC does not catalyze the incorporation of a solvent proton at the thiol-functionalized carbon of the product **2**, suggesting that the dihydroflavin intermediate is protected from solvent and presumably also from oxygen (*4*). Unlike the native enzyme, the C173S mutant protein is unable to oxidize the thiol moieties of the product **2** and *P*PanΔSH (**3**). As a result *P*PanΔSH does not function as an inhibitor of the mutant enzyme.

CONCLUSION

This study describes the design and characterization of an efficient mechanism-based inhibitor (*P*PanΔSH (**3**)) of human *P*PC-DC. This inhibitor is activated by oxidation to the electrophilic cyclopropyl thioaldehyde **22**, which then alkylates Cys^{173} to generate the stable enethiolate **23**. This suggests that Cys^{173} functions as the active site acid that protonates the enethiolate **7**. When Cys^{173} is exchanged for the weaker acid serine by mutagenesis, the enethiolate also accumulates. Our experiments suggest that enethiolate protonation is essential for reduction and point to the availability of an active site residue that can perform such a protonation of the intermediate as the major mechanistic difference between catalysis of a simple decarboxylation and an oxidative decarboxylation in this family of enzymes.

ACKNOWLEDGMENT

The authors thank André Venter for help with ESI-MS analyses, and Brian Lawhorn for helpful discussions.

REFERENCES

1. Begley, T. P., Kinsland, C., and Strauss, E. (2001) The biosynthesis of Coenzyme A in bacteria, *Vitam. Horm. 61*, 157−171.
2. Kupke, T., Hernandez-Acosta, P., Steinbacher, S., and Culianez-Macia, F. A. (2001) *Arabidopsis thaliana* flavoprotein AtHAL3a catalyzes the decarboxylation of 4′-phosphopantothenoylcysteine to 4′-phosphopantetheine, a key step in coenzyme A biosynthesis, *J. Biol. Chem. 276*, 19190−19196.
3. Daugherty, M., Polanuyer, B., Farrell, M., Scholle, M., Lykidis, A., De Crécy-Lagard, V., and Osterman, A. (2002) Complete

Reconstitution of the Human Coenzyme A Biosynthetic Pathway via Comparitive Genomics, *J. Biol. Chem. 277*, 21431−21439.
4. Strauss, E., and Begley, T. P. (2001) Mechanistic Studies on Phosphopantothenoylcysteine Decarboxylase, *J. Am. Chem. Soc. 123*, 6449−6450.
5. Kupke, T., Uebele, M., Schmid, D., Jung, G., Blaesse, M., and Steinbacher, S. (2000) Molecular characterization of lantibiotic-synthesizing enzyme EpiD reveals a function for bacterial Dfp proteins in coenzyme A biosynthesis, *J. Biol. Chem. 275*, 31838−31846.
6. Strauss, E., and Begley, T. P. (2003) Stereochemical studies on phosphopantothenoylcysteine decarboxylase from *Escherichia coli*, *Bioorg. Med. Chem. Lett. 13*, 339−342.
7. Palfey, B. A., and Massey, V. (1998) Flavin-dependent Enzymes, in *Comprehensive Biological Catalysis* (Sinnott, M., Ed.) pp 83−154, Academic Press, San Diego, CA.
8. Miller, S. M., Massey, V., Ballou, D., Williams, C. H., Jr., Distefano, M. D., Moore, M. J., and Walsh, C. T. (1990) Use of a site-directed triple mutant to trap intermediates: demonstration that the flavin C(4a)-thiol adduct and reduced flavin are kinetically competent intermediates in mercuric ion reductase, *Biochemistry 29*, 2831−2841.
9. Thorpe, C., and Williams, C. H., Jr. (1981) Lipoamide dehydrogenase from pig heart. Pyridine nucleotide induced changes in monoalkylated two-electron reduced enzyme, *Biochemistry 20*, 1507−1513.
10. Kupke, T., Kempter, C., Jung, G., and Goetz, F. (1995) Oxidative decarboxylation of peptides catalyzed by flavoprotein EpiD. Determination of substrate specificity using peptide libraries and neutral loss mass spectrometry, *J. Biol. Chem. 270*, 11282−11289.
11. Kupke, T., Stevanovic, S., Sahl, H. G., and Goetz, F. (1992) Purification and characterization of EpiD, a flavoprotein involved in the biosynthesis of the lantibiotic epidermin, *J. Bacteriol. 174*, 5354−5361.
12. Majer, F., Schmid, D. G., Altena, K., Bierbaum, G., and Kupke, T. (2002) The flavoprotein MrsD catalyzes the oxidative decarboxylation reaction involved in formation of the peptidoglycan biosynthesis inhibitor mersacidin, *J. Bacteriol. 184*, 1234−1243.
13. Xie, L., and van der Donk, W. A. (2004) Post-translational modifications during lantibiotic biosynthesis, *Curr. Opin. Chem. Biol. 8*, 498−507.
14. Hernandez-Acosta, P., Schmid, D. G., Jung, G., Culianez-Macia, F. A., and Kupke, T. (2002) Molecular characterization of the *Arabidopsis thaliana* flavoprotein AtHAL3a reveals the general reaction mechanism of 4′-phosphopantothenoylcysteine decarboxylases, *J. Biol. Chem. 277*, 20490−20498.
15. Kupke, T. (2001) Molecular characterization of the 4′-phosphopantothenoylcysteine decarboxylase domain of bacterial Dfp flavoproteins, *J. Biol. Chem. 276*, 27597−27604.
16. Albert, A., Martinez-Ripoll, M., Espinosa-Ruiz, A., Yenush, L., Culianez-Macia, F. A., and Serrano, R. (2000) The X-ray structure of the FMN-binding protein AtHal3 provides the structural basis for the activity of a regulatory subunit involved in signal transduction, *Structure 8*, 961−969.
17. Blaesse, M., Kupke, T., Huber, R., and Steinbacher, S. (2000) Crystal structure of the peptidyl-cysteine decarboxylase EpiD complexed with a pentapeptide substrate, *EMBO J. 19*, 6299−6310.
18. Steinbacher, S., Hernandez-Acosta, P., Bieseler, B., Blaesse, M., Huber, R., Culianez-Macia, F. A., and Kupke, T. (2003) Crystal Structure of the Plant PPC Decarboxylase AtHAL3a Complexed with an Ene-thiol Reaction Intermediate, *J. Mol. Biol. 327*, 193−202.
19. Karthikeyan, S., Zhao, Z., Kao, C., Zhou, Q., Tao, Z., Zhang, H., and Liu, H.-w. (2004) Structural analysis of 1-aminocyclopropane-1-carboxylate deaminase: Observation of an aminyl intermediate and identification of Tyr294 as the active-site nucleophile, *Angew. Chem., Int. Ed. 43*, 3425−3429.
20. Zhao, Z., Chen, H., Li, K., Du, W., He, S., and Liu, H.-w. (2003) Reaction of 1-Amino-2-methylenecyclopropane-1-carboxylate with 1-Aminocyclopropane-1-carboxylate Deaminase: Analysis and Mechanistic Implications, *Biochemistry 42*, 2089−2103.
21. Liu, H.-W. (1998) Coenzyme B6 dependent novel bond cleavage reactions, *Pure Appl. Chem. 70*, 9−16.
22. Li, K., Du, W., Que, N. L. S., and Liu, H.-w. (1996) Mechanistic studies of 1-aminocyclopropane-1-carboxylate deaminase: Unique covalent catalysis by coenzyme B_6, *J. Am. Chem. Soc. 118*, 8763−8764.
23. MacInnes, I., Nonhebel, D. C., Orszulik, S. T., Suckling, C. J., and Wrigglesworth, R. (1980) exo-Bicyclo[4.1.0]heptane-7-methanol: a novel latent inhibitor of liver alcohol dehydrogenase, *J. Chem. Soc., Chem. Commun.* 1068−1069.
24. MacInnes, I., Nonhebel, D. C., Orszulik, S. T., Suckling, C. J., and Wrigglesworth, R. (1983) Latent inhibitors. Part 3. The inhibition of lactate dehydrogenase and alcohol dehydrogenase by cyclopropane-containing compounds, *J. Chem. Soc., Perkin Trans. 1*, 2771−2776.
25. Ner, S. K., Suckling, C. J., Bell, A. R., and Wrigglesworth, R. (1987) Inhibition of carboxypeptidase by cyclopropane-containing peptides, *J. Chem. Soc., Chem. Commun.* 480−482.
26. Suckling, C. J. (1988) The cyclopropyl group in research on the mechanism and inhibition of enzymes, *Angew. Chem., Int. Ed. Engl. 27*, 537−552.
27. Haddow, J., Suckling, C. J., and Wood, H. C. S. (1989) Latent inhibitors. Part 5. Latent inhibition of dihydrofolate reductase by a pteridine-spiro-cyclopropane *J. Chem. Soc., Perkin Trans. 1*, 1297−1304.
28. Fraser, W., Suckling, C. J., and Wood, H. C. S. (1990) Latent inhibitors. Part 7. Inhibition of dihydroorotate dehydrogenase by spirocyclopropanobarbiturates, *J. Chem. Soc., Perkin Trans. 1*, 3137−3144.
29. McGill, J., Rees, L., Suckling, C. J., and Wood, H. C. S. (1992) Latent inhibitors. Part 8. Synthesis and evaluation of some mechanism-based inhibitors of dihydrofolate reductase, *J. Chem. Soc., Perkin Trans. 1*, 1299−1304.
30. Kemp, A., Ner, S. K., Rees, L., Suckling, C. J., Tedford, M. C., Bell, A. R., and Wrigglesworth, R. (1993) Latent inhibitors. Part 9. Substrate activated time-dependent inhibition of carboxypeptidase A by aminocyclopropanecarboxylic acid derivatives and analogs, *J. Chem. Soc., Perkin Trans. 2*, 741−748.
31. Silverman, R. B., Ding, C. Z., Borrillo, J. L., and Chang, J. T. (1993) Mechanism-based enzyme inactivation via a diactivated cyclopropane intermediate, *J. Am. Chem. Soc. 115*, 2982−2983.
32. Silverman, R. B., Lu, X., Blomquist, G. D., Ding, C. Z., and Yang, S. (1997) Inactivation of monoamine oxidase B by benzyl 1-(aminomethyl)cyclopropane-1-carboxylate, *Bioorg. Med. Chem. 5*, 297−304.
33. Danishefsky, S. (1979) Electrophilic cyclopropanes in organic synthesis, *Acc. Chem. Res. 12*, 66−72.
34. Kupke, T., and Goetz, F. (1997) The enethiolate anion reaction products of EpiD. pK_a value of the enethiol side chain is lower than that of the thiol side chain of peptides, *J. Biol. Chem. 272*, 4759−4762.
35. Moffatt, J. G., and Khorana, H. G. (1961) Nucleoside polyphosphates. XII. The total synthesis of coenzyme A, *J. Am. Chem. Soc. 83*, 663−675.
36. Strauss, E., Kinsland, C., Ge, Y., McLafferty, F. W., and Begley, T. P. (2001) Phosphopantothenoylcysteine synthetase from *Escherichia coli*. Identification and characterization of the last unidentified coenzyme A biosynthetic enzyme in bacteria, *J. Biol. Chem. 276*, 13513−13516.
37. O'Brien, W. E. (1976) A continuous spectrophotometric assay for argininosuccinate synthetase based on pyrophosphate formation, *Anal. Biochem. 76*, 423−430.
38. Strauss, E., and Begley, T. P. (2002) The Antibiotic Activity of *N*-Pentylpantothenamide Results from Its Conversion to Ethyldethia-Coenzyme A, a Coenzyme A Antimetabolite, *J. Biol. Chem. 277*, 48205−48209.
39. Wilm, M., and Mann, M. (1996) Analytical Properties of the Nanoelectrospray Ion Source, *Anal. Chem. 68*, 1−8.
40. Beu, S. C., Senko, M. W., Quinn, J. P., Wampler, F. M., III, and McLafferty, F. W. (1993) Fourier transform electrospray instrumentation for tandem high-resolution mass spectrometry of large molecules, *J. Am. Soc. Mass Spectrom. 4*, 557−565.
41. Horn, D. M., Zubarev, R. A., and McLafferty, F. W. (2000) Automated reduction and interpretation of high-resolution electrospray mass spectra of large molecules, *J. Am. Soc. Mass Spectrom. 11*, 320−332.
42. Sklenak, S., Apeloig, Y., and Rappoport, Z. (2000) Equilibria of simple thioenol/thiocarbonyl pairs. Comparison with the oxygen analogues and with the parent selenium and tellurium systems. A theoretical study *J. Chem. Soc., Perkin Trans. 2*, 2269−2279.
43. Kresge, A. J., and Meng, Q. (1998) 2,4,6-Trimethylthioacetophenone and Its Enol. The First Quantitative Characterization of a Simple Thiocarbonyl System in Aqueous Solution, *J. Am. Chem. Soc. 120*, 11830−11831.

44. Kempter, C., Kupke, T., Kaiser, D., Metzger, J. W., and Jung, G. (1996) Thioenols from peptidyl cysteines: oxidative decarboxylation of a ^{13}C-labeled substrate, *Angew. Chem., Int. Ed. Engl. 35*, 2104−2107.
45. Manoj, N., and Ealick, S. E. (2003) Unusual space-group pseudosymmetry in crystals of human phosphopantothenoylcysteine decarboxylase, *Acta Crystallogr., Sect. D: Biol. Crystallogr. 59*, 1762−1766.
46. Silverman, R. B. (1995) Mechanism-based enzyme inactivators, *Methods Enzymol. 249*, 240−283.

BI048340A